

Radiation of a TM mode from an open end of a three-layer dielectric capillary

Sergey N. Galyamin and Alexandr M. Altmark

Citation: Chin. Phys. B, 2024, 33 (**7**): 074102. DOI: 10.1088/1674-1056/ad3ef7
Journal homepage: http://cpb.iphy.ac.cn; http://iopscience.iop.org/cpb

What follows is a list of articles you may be interested in

On-chip ultrafast stackable dielectric laser positron accelerator

Bin Sun(孙斌), Yangfan He(何阳帆), Chenhao Pan(潘晨浩), Sijie Fan(樊思劼), Du Wang(王度), Shaoyi Wang(王少义), and Zongqing Zhao(赵宗清)
Chin. Phys. B, 2024, 33 (**3**): 034101. DOI: 10.1088/1674-1056/ad188e

Wideband low-scattering metasurface with an in-band reconfigurable transparent window

Ying Zhu(朱瑛), Weixu Yang(杨维旭), Kun Duan(段坤), Tian Jiang(姜田), Junming Zhao(赵俊明), Ke Chen(陈克), and Yijun Feng(冯一军)
Chin. Phys. B, 2024, 33 (**2**): 024102. DOI: 10.1088/1674-1056/ad0119

Cherenkov terahertz radiation from Dirac semimetals surface plasmon polaritons excited by an electron beam

Tao Zhao(赵陶), Zhenhua Wu(吴振华)
Chin. Phys. B, 2020, 29 (**3**): 034101. DOI: 10.1088/1674-1056/ab6840

Polarization-dependent efficient Cherenkov radiation at visible wavelengths in hollow-core photonic crystal fiber cladding

Shen Xiang-Wei (申向伟), Yuan Jin-Hui (苑金辉), Sang Xin-Zhu (桑新柱), Yu Chong-Xiu (余重秀), Rao Lan (饶岚), Xia Min (夏民), Han Ying (韩颖), Xia Chang-Ming (夏长明), Hou Lan-Tian (侯蓝田), Wu Zhong-Chao (吴中超), He Xiao-Liang (何晓亮)
Chin. Phys. B, 2013, 22 (**1**): 014102. DOI: 10.1088/1674-1056/22/1/014102

Highly efficient Cherenkov radiation generation in the irregular point of hollow-core photonic crystal fiber

Shen Xiang-Wei (申向伟), Yuan Jin-Hui (苑金辉), Sang Xin-Zhu (桑新柱), Yu Chong-Xiu (余重秀), Rao Lan (饶兰), Xia Min (夏民), Han Ying (韩颖), Xia Chang-Ming (夏长明), Hou Lan-Tian (侯蓝田)
Chin. Phys. B, 2012, 21 (**11**): 114102. DOI: 10.1088/1674-1056/21/11/114102

Radiation of a TM mode from an open end of a three-layer dielectric capillary

Sergey N. Galyamin[1,†] and Alexandr M. Altmark[2]

[1] *St. Petersburg State University, 7/9 Universitetskaya nab., St. Petersburg* 199034, *Russia*
[2] *St. Petersburg Electrotechnical University "LETI", 5 Professora Popova, St. Petersburg* 197022, *Russia*

(Received 21 December 2023; revised manuscript received 28 March 2024; accepted manuscript online 16 April 2024)

Modern trends in beam-driven radiation sources include the interaction of Cherenkov wakefields in open-ended circular waveguides with complicated dielectric linings, with a three-layer dielectric capillary recently proposed to reduce radiation divergence being a representative example [*Opt. Lett.* **45** 5416 (2020)]. We present a rigorous approach that allows for an analytical description of the electromagnetic processes that occur when the structure is excited by a single waveguide TM mode. In other words, the corresponding canonical waveguide diffraction problem is solved in a rigorous formulation. This is a continuation of our previous papers which considered simpler cases with a homogeneous or two-layer dielectric filling. Here we use the same analytical approach based on the Wiener–Hopf–Fock technique and deal with the more complicated case of a three-layer dielectric lining. Using the obtained rigorous solution, we discuss the possibility of manipulating the far-field radiation pattern using a third layer made of a low permittivity material.

Keywords: diffraction radiation, open-ended waveguide, Wiener–Hopf technique, Cherenkov radiation

PACS: 41.20.Jb, 42.25.Fx, 41.60.–m, 41.60.Bq **DOI:** 10.1088/1674-1056/ad3ef7

1. Introduction

Dielectric-lined open-ended waveguide structures have recently been considered as an extremely promising option for a variety of applications based on the Cherenkov effect. In the context of this paper, we can mention a certain success in the field of dielectric wakefield acceleration,[1–6] as well as in the development of high-power narrow-band radiation sources including those for terahertz (THz) frequencies.[7–10] A typical structure for these applications is a dielectric capillary, which is a circular waveguide with a dielectric layer and an axial channel for the passage of bunches. However, much more complex structures including those incorporating metamaterials have also been considered.[11,12] Recently, a promising modification to the aforementioned two-layer capillary has been proposed.[13] The authors of Ref. [13] numerically investigated the possibilities to enhance the directivity and reduce the reflection of the capillary-based beam-driven THz radiation source by adding a third layer with a permittivity just slightly larger than unity. However, an "opposite" idea of using a thin third layer of high-permittivity material for tunable wakefield acceleration structure in the GHz frequency range has also been discussed.[14] The third layer is made of a ferroelectric material whose permittivity can be sensitive to changes in both temperature and DC bias voltage. Experimental verification of this idea has been particularly successful.[15] Modern ferroelectrics like strontium titanate can even be used at THz frequencies where their dielectric permittivity is sufficiently high and can be changed over a wide range by an external DC electric field.[16]

For further development of the discussed topics, a rigorous approach allowing the analytical study of both the radiation from such an open-ended capillary and its excitation by an external source (bunch or electromagnetic pulse) would be extremely useful. In our recent papers,[17,18] we presented an efficient rigorous method for solving circular open-ended waveguide diffraction problems and illustrated this method using the case of a uniform dielectric filling and a two-layer lining of the waveguide. Here we deal with a more complicated geometry offered in Ref. [13] and internal excitation by a single waveguide TM mode. The presented technique can be directly applied to the radiation of the CR wakefield generated behind the moving charge in the form of a slow waveguide mode. Moreover, the presented rigorous solution can potentially be extended to a beam-driven case (similar to what has been done for "embedded" structures[19]).

Besides the above-mentioned practical importance, the present work also contributes to the development of rigorous diffraction theory, since it deals with a canonical problem, i.e., a relatively simple geometric structure (so-called "canonical structure") excited by a simple free or guided wave. A series of related problems associated with an open end discontinuity[20–38] or a cross-sectional discontinuity[39,40] in waveguides and resonators can be mentioned. However, the diffraction problem with a canonical structure discussed in this paper has not been rigorously investigated so far.

In this paper we discuss and further develop the idea of Ref. [13], where the third layer of the structure has a dielectric permittivity just slightly above unity. We show that increasing the thickness of this additional layer does indeed significantly

†Corresponding author. E-mail: s.galyamin@spbu.ru

© 2024 Chinese Physical Society and IOP Publishing Ltd

reduce the width of the main lobe of the far-field radiation pattern and thus increases the radiated power for the fundamental Cherenkov mode. We also move forward by considering higher order Cherenkov modes (which were not discussed at all in Ref. [13]), which allows the radiation frequency to be shifted into the THz range for mm-sized capillaries.

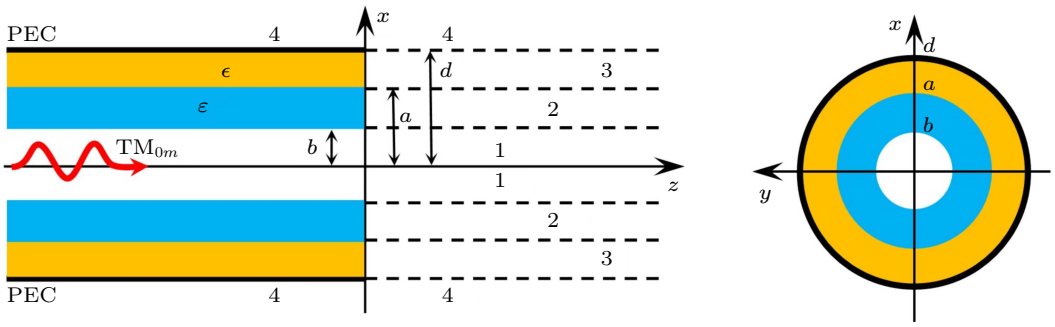


Fig. 1. Geometry of a three-layer problem.

The paper is organized as follows. After the introduction, we present the problem formulation and main notations in Section 2. Section 3 contains numerical results (radiation patterns, S parameters) for the structure proposed in Ref. [13] and corresponding discussion. In Section 4, we give the detailed solution of the problem for those interested in analytical derivations and the mathematical essence of the approach used.

2. Problem formulation

We consider an open-ended semi-infinite cylindrical waveguide with radius d lined with a dielectric $\varepsilon > 1$ of thickness $a-b$ and having a layer of thickness $d-a$ of dielectric $\epsilon > 1$ near the waveguide wall, see Fig. 1 (a cylindrical frame ρ, φ, z is used). The region outside the waveguide ($z > 0$ and $z < 0$, $\rho > d$) and the inner channel ($z < 0$, $\rho < b$) are filled with vacuum. The walls of the waveguide have an ideal electrical conductivity (PEC). The method of solution is the same as in Refs. [17,18].

A φ-symmetric TM problem is considered in the harmonic regime with the time dependence in the form

$$H_\varphi(\rho,z,t) = H_{\omega\varphi}(\rho,z)\exp(-\mathrm{i}\omega t). \tag{1}$$

This problem is formulated for the magnitude $H_{\omega\varphi}$, other nonzero field components can be derived as follows:

$$E_{\omega\rho} = \frac{1}{\mathrm{i}k_0\tilde{\varepsilon}}\frac{\partial H_{\omega\varphi}}{\partial z},\quad E_{\omega z} = \frac{\mathrm{i}}{k_0\tilde{\varepsilon}}\left(\frac{H_{\omega\varphi}}{\rho} + \frac{\partial H_{\omega\varphi}}{\partial \rho}\right), \tag{2}$$

where $\tilde{\varepsilon} = 1$, ε or ϵ depending on the region. In particular, we have $E_{\omega z} = 0$ for $\rho = d$, $z < 0$.

We assume that a single symmetric TM_{0l} waveguide mode is incident on the orthogonal open end of the waveguide:

$$H^{(i)}_{\omega\varphi} = M^{(i)}\,\mathrm{e}^{\,\mathrm{i}k_{zl}z}\begin{cases} J_1(\rho\sigma_l)/\sigma_l, & \text{for } \rho < b,\\ \dfrac{J_1(b\sigma_l)}{\sigma_l}\dfrac{\psi_l(\rho)}{\psi_l(b)}, & \text{for } b < \rho < a,\\ \dfrac{J_1(b\sigma_l)}{\sigma_l}\dfrac{\psi_l(a)}{\psi_l(b)}\dfrac{\psi_{0l}(\rho)}{\psi_{0l}(a)}, & \text{for } a < \rho < d, \end{cases} \tag{3}$$

where $M^{(i)}$ is an arbitrary amplitude constant,

$$\begin{aligned}
&\psi_{0m}(\xi) = J_1(\xi\chi_m)Y_0(d\chi_m) - Y_1(\xi\chi_m)J_0(d\chi_m),\\
&\psi_m(\xi) = J_1(\xi s_m)\varphi_{2m} - Y_1(\xi s_m)\varphi_{1m},\\
&\varphi_{1m} = \sigma_m J_0(b\sigma_m)J_1(bs_m) - s_m\varepsilon^{-1}J_1(b\sigma_m)J_0(bs_m),\\
&\varphi_{2m} = \sigma_m J_0(b\sigma_m)Y_1(bs_m) - s_m\varepsilon^{-1}J_1(b\sigma_m)Y_0(bs_m),
\end{aligned} \tag{4}$$

where J_ν and Y_ν are the Bessel and Neumann functions of ν-th order, respectively, transverse wave numbers σ_m, s_m, and χ_m are determined by the following dispersion equation:

$$\det\hat{M} = 0, \tag{5}$$

$$\hat{M} = \begin{pmatrix} \varphi_{1m} & \varphi_{2m} & 0 & 0\\ J_1(as_m) & Y_1(as_m) & -J_1(a\chi_m) & -Y_1(a\chi_m)\\ \dfrac{s_m J_0(as_m)}{\varepsilon} & \dfrac{s_m Y_0(as_m)}{\varepsilon} & \dfrac{-\chi_m J_0(a\chi_m)}{\epsilon} & \dfrac{-\chi_m Y_0(a\chi_m)}{\epsilon}\\ 0 & 0 & J_0(d\chi_m) & Y_0(d\chi_m) \end{pmatrix}, \tag{6}$$

longitudinal wave number k_z is connected with σ_m, s_m, and χ_m as follows:

$$k_{zm} = \sqrt{k_0^2 - \sigma_m^2} = \sqrt{k_0^2\varepsilon - s_m^2} = \sqrt{k_0^2\epsilon - \chi_m^2},\ \ \mathrm{Im}k_{zm} > 0, \tag{7}$$

$k_0 = \omega/c + \mathrm{i}\delta$ ($\delta \to 0$, which is equivalent to an infinitely small dissipation an all areas), c is the light speed in vacuum. From Eq. (7) one can express both s_m and χ_m through σ_m and obtain the dispersion relation with respect to a single variable σ_m. Note that Eq. (3) transforms to the corresponding mode of a two-layer waveguide of radius d (Ref. [18]) for $\epsilon \to \varepsilon$. The problem is to find diffracted electromagnetic field both inside and outside the waveguide which satisfies ordinary boundary conditions on all boundaries and at the infinity together with the incident field (3). Exact solution will be given in Section 4.

3. Numerical results

For practical applications of the discussed three-layer structure in the area of beam-driven radiation sources, far-field

radiation patterns are of most importance. These patterns are obtained as follows. The integral $I_q^{(4)}(\rho,z)$ from Section 4 can be calculated asymptotically in the far-field area: $k_0R \gg 1$, $\theta \gg 1/\sqrt{k_0R}$, $\pi-\theta \gg 1/\sqrt{k_0R}$ (hereafter it is always supposed that R is so large that limits values of θ lie in area 4). In our case, the saddle point is isolated and we obtain[17]

$$I_m^{(4)}(\rho,z) \approx I_m^{(4a)}(\rho,z) = \pi a \frac{e^{ik_0R}}{R} \frac{\kappa_-(k_0\cos\theta)}{G_+(k_0\cos\theta)} \frac{2J_0(ak_0\sin\theta)}{k_0\cos\theta-\alpha_q}. \tag{8}$$

This expression should be substituted to the formula for $H_{\omega\varphi}^{(4)}(\rho,z)$ to obtain the far field in the region 4. For large enough R, areas 1, 2 and 3 (see Fig. 1) occupy relatively small region of θ therefore it is sufficient to consider radiation in region 4 only.

It is also useful to consider the electromagnetic power carried by the incident mode and any reflected propagating mode through the waveguide cross section. For this, z component of the Poynting vector averaged over the period $2\pi/\omega$ is calculated (the overline means complex conjugation)

$$S_z^{\text{av}} = \frac{c}{8\pi}\text{Re}[E_{\omega\rho}\overline{H_{\omega\varphi}}], \tag{9}$$

and integrated over the cross section:

$$\Sigma = 2\pi\int_0^d S_z^{\text{av}}\rho\,\text{d}\rho. \tag{10}$$

Then the corresponding S parameters are constructed:

$$S_{ml} = \sqrt{\Sigma_m^{(r)}/\Sigma^{(i)}}, \tag{11}$$

which can also be expressed in dB, $S_{ml}^{\text{dB}} = 20\log S_{ml}$.

For the calculations presented below, the mode frequency was chosen to be equal to the frequency of the Cherenkov radiation (CR) mode f_l^{CR} (l is a mode number) produced by a moving charged particle bunch with a given Lorentz factor γ (note that a relativistic case $\gamma \gg 1$ is considered in the following, which is of most practical importance). To find the set of Cherenkov frequencies $\{f_m^{\text{CR}}\}$, we should solve numerically the dispersion equation (5) with respect to the frequency. For this, σ_m, s_m and χ_m in $\hat{M}$ [Eq. (6)] should be also expressed through the frequency $f=\omega/(2\pi)$ using Eq. (7) and the following relation:

$$k_{zm} = \omega_m(c\beta)^{-1}, \tag{12}$$

where $c\beta$ is a charge velocity, $\beta^2 = 1-\gamma^{-2}$. Equation (12) means a synchronicity between a moving charge and the m-th waveguide mode. In other words, Eq. (12) means that for given frequency f_m^{CR} a mode with number m is slow and its phase velocity equals the charge velocity, which holds for CR modes.[41] If $M^{(i)}$ is chosen appropriately, an incident mode (3) for $\{f_l^{\text{CR}}\}$ corresponds to the l-th mode of the wakefield generated in the structure by a charged particle bunch. If a bunch train with proper spatial modulation is used instead of a single bunch, then high-order CR modes ($l>1$) can be in principle generated separately, see Section III-B in Ref. [19].

Next, we discuss an application of the developed theory to a three-layer structure taken from Ref. [13]. First we present numerical results for exact parameters used in this paper. According to Ref. [13], dielectric permittivity of the third layer satisfies $\epsilon > 1$ but is close to unity, $\epsilon - 1 \ll 1$. We suppose that frequency equals the Cherenkov frequency with number l therefore the incident TM-mode (3) simulates the l-th Cherenkov mode of a wakefield generated by a charged particle bunch. Far-field patterns are calculated using Eq. (8) and the formula for $H_{\omega\varphi}^{(4)}$ from Section 4.

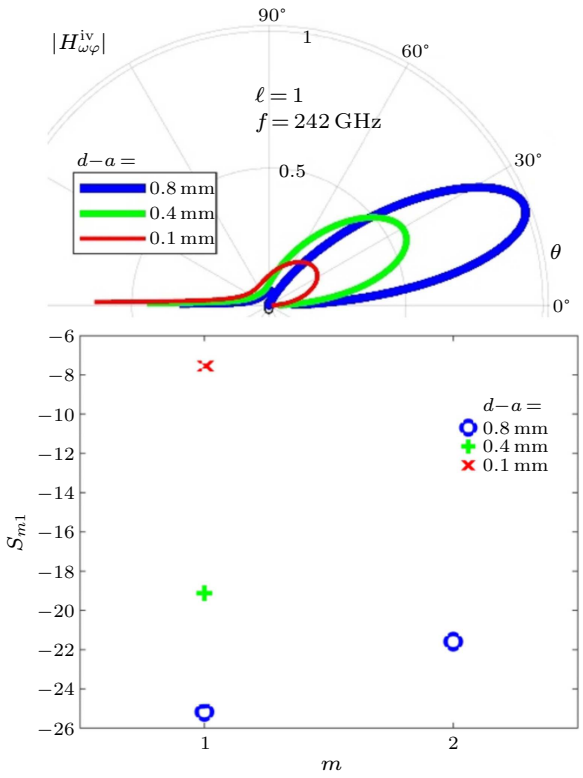


Fig. 2. Normalized far-field patterns (top) and S-parameters (bottom) for the 1-st Cherenkov mode (f_1^{CR} is indicated in the plot, the curves are normalized to the maximum of the curve for $d-a=0.8$ mm) exiting the three-layer structure. Parameters: $b=0.4$ mm, $a=0.55$ mm, $\varepsilon=3.8$ (fused silica), $\epsilon=1.01$, $\gamma=10$, thickness of the third layer $d-a$ is indicated in the legend.

The top plot in Fig. 2 shows how the radiation of the fundamental Cherenkov mode ($l=1$) changes with an increase in the thickness of the third layer. As one can see, the position of radiation maximum (39°, 35°, 21°) and its width ($2\Delta\theta_{0.7} = 52°, 35°, 25°$) decrease twice while field magnitude increases 2.5 times with an increase in the thickness of the third layer from 0.1 mm to 0.8 mm. Reflection described by S_{11} and shown at the bottom plot in Fig. 3 also decreases essentially from approximately −8 dB to −25 dB. Note that the change in Cherenkov frequency f_1^{CR} with $(d-a)$ is negligibly in this case. The results shown indicate both the correctness and fruitfulness of the idea presented in Ref. [13].

However, a capillary possessing the fundamental Cherenkov mode with a frequency lying even in the lower

part of the THz region is sub-mm in transverse direction (this is a very thin capillary). Therefore, it is rather complicated to manufacture. Moreover, the transverse size of the bunch that can pass through such a capillary should be even smaller, therefore complicating the practical realization of the scheme considerably. To achieve the same frequencies, an approximately one order larger structure (i.e., a much thicker capillary) can be used if high-order Cherenkov modes are generated and radiated.[7] As is well known, high-order modes can be generated in dielectric-lined waveguides by a charged particle bunch with proper charge modulation, i.e., by a bunch train.[42] Parameters of the train can be chosen so that the bunch train spectrum has the expressed maximum exactly at the required Cherenkov frequency f_l^{CR}, therefore the corresponding CR mode can be generated separately (see, for example, Fig. 9 in Ref. [19] for details). It is worth noting that CST simulation similar to that performed in Ref. [13] is much more complicated for high-order modes and is therefore rarely presented in publications. However, the analytical approach presented in this paper allows for easily calculating corresponding patterns.

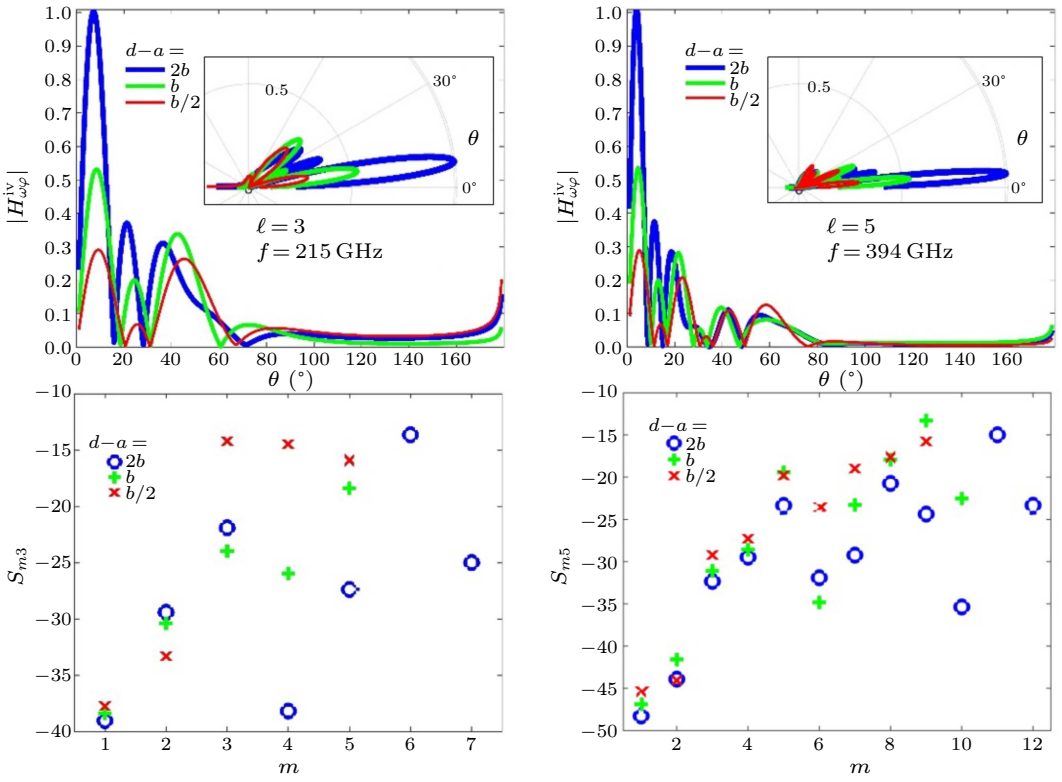


Fig. 3. Normalized far-field patterns (top) and S-parameters (bottom) for high-order Cherenkov modes (f_l^{CR} is indicated in the plots, the curves are normalized to the maximum of the curve for $d-a=2b$) exiting the three-layer structure. Parameters: $a=0.24$ cm, $b=a/3$, $\varepsilon=2$ (Teflon), $\epsilon=1.01$, $\gamma=10$, thickness of the third layer $d-a$ is indicated in the legend.

Figure 3 (top plots) shows the normalized far-field patterns for the case of a thick (mm-sized) capillary driven by Cherenkov modes with numbers $l=3$ and $l=5$. As one can see, in all the cases radiation patterns possess lateral (parasitic) lobes especially for relatively small thickness of the addition layer ($d-a=b/2$). However, with an increase in $d-a$ the main lobe increases considerably and the role of mentioned parasitic lobes decreases so that it becomes inessential for $d-a=2b$. Moreover, magnitude of the main lobe increases $2\div4$ times (depending on l) with an increase in $d-a$ from $b/2$ to $2b$. Reflection of the incident mode S_{ll} (S parameters are shown in bottom plots of Fig. 3) is relatively small even for $d-a=b/2$ (less than -15 dB) and becomes even smaller for thicker addition layer ($d-a=2b$). Angle of the main lobe decreases with an increase in number of the excited Cherenkov mode. Overall, the presented results indicate potential applicability of the discussed structure for realization of a beam-driven THz radiation source in the case of relatively thick capillary and high-order Cherenkov modes which can be generated by short enough charged particle bunch. For an enough thick additional layer with $0<\epsilon-1\ll1$ a single-lobe radiation pattern with low reflection may be achieved.

It is also of interest to compare the obtained analytic results with simulated ones. Figure 4 shows a comparison between S-parameters calculated for the discussed three-layer structure (parameters are the same as those in Fig. 3, left column, the third layer thickness is $d-a=2b$) when excited by the 3rd Cherenkov mode. Blue o markers correspond to the S-parameters obtained via a rigorous analytic approach presented in this paper. Red cross markers correspond to the S-parameters simulated using the 2-D axisymmetric frequency domain solver of COMSOL Multiphysics (RF module). Sim-

ilar to Refs. [17,18], an input end of the waveguide was supported by a series of numerical ports, one separate port for each propagating mode (the port that corresponds to the incident mode was set to be active). The corresponding eigenmodes were determined numerically, with analytically calculated longitudinal wavenumbers k_{zm} being used as guess values. An open end of the waveguide was surrounded by a hemisphere with a scattering boundary condition applied. The outer waveguide wall was set to be a perfect electrical conductor (PEC). As one can see from Fig. 4, the coincidence between these two sets of S-parameters is close to excellent, thus proving both the presented theory and the correctness of the COMSOL simulation procedure.

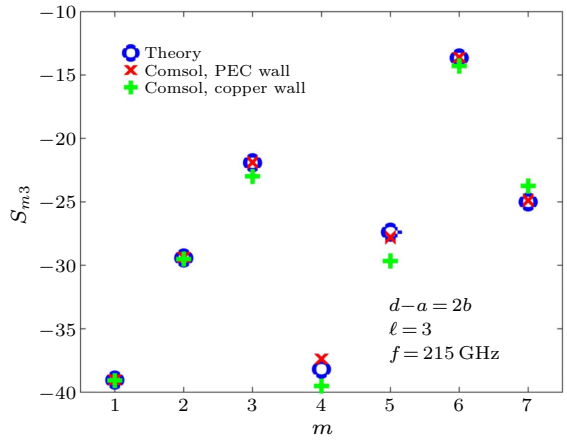


Fig. 4. S-parameters for the 3rd Cherenkov mode exiting the three-layer structure with the same parameters as in Fig. 3, left column ($d-a=2b$) calculated using the presented analytic approach (blue o markers), simulated in COMSOL with PEC outer wall (red cross markers) and simulated in COMSOL with copper outer wall of thickness $a/20$ (green plus markers).

In addition, green plus markers in Fig. 4 show the COMSOL-simulated S-parameters in the case where the outer waveguide wall is made of copper of finite thickness. As one can see, realistic wall material affects S-parameters insignificantly: for the worst case (S_{53}) the difference is about 2 dB on the -27 dB level.

4. General solution of the problem

Here we present the rigorous solution of the problem. The reflected field in the area inside the waveguide ($z<0$, $\rho<a$) is decomposed into a series of TM modes propagating in the opposite direction:

$$H^{(r)}_{\omega\varphi}=\sum_{m=0}^{\infty}M_m\,\mathrm{e}^{-\mathrm{i}k_{zm}z}\begin{cases}J_1(\rho\sigma_m)/\sigma_m, & \text{for } \rho<b,\\ \frac{J_1(b\sigma_m)}{\sigma_m}\frac{\psi_m(\rho)}{\psi_m(b)}, & \text{for } b<\rho<a,\\ \frac{J_1(b\sigma_m)}{\sigma_m}\frac{\psi_m(a)}{\psi_m(b)}\frac{\psi_{0m}(\rho)}{\psi_{0m}(a)}, & \text{for } a<\rho<d,\end{cases}\tag{13}$$

where $\{M_m\}$ are unknown "reflection coefficients" that should be determined. Note that since both the structure and the excitation (3) are uniform in φ, only symmetric TM modes are taken into account in the reflected field.

The area outside the waveguide is divided into three subareas 1, 2, 3, and 4 (see Fig. 1), where the field is described by Helmholtz equation:

$$\Big[\frac{\partial^2}{\partial z^2}+\frac{\partial^2}{\partial\rho^2}+\frac{1}{\rho}\frac{\partial}{\partial\rho}+\Big(k_0^2-\frac{1}{\rho^2}\Big)\Big]H^{(1,2,3,4)}_{\omega\varphi}=0.\tag{14}$$

We introduce functions $\Psi_{\pm}(\rho,\alpha)$ (hereafter subscripts $\pm$ mean that the function is holomorphic and free of poles and zeros in areas $\mathrm{Im}\,\alpha>-\delta$ and $\mathrm{Im}\alpha<\delta$, correspondingly):

$$\Psi^{(1,2,3,4)}_{+}(\rho,\alpha)=(2\pi)^{-1}\int_0^{\infty}\mathrm{d}zH^{(1,2,3,4)}_{\omega\varphi}(\rho,z)\,\mathrm{e}^{\mathrm{i}\alpha z},\tag{15}$$

$$\Psi^{(4)}_{-}(\rho,\alpha)=(2\pi)^{-1}\int_{-\infty}^{0}\mathrm{d}zH^{(4)}_{\omega\varphi}(\rho,z)\,\mathrm{e}^{\mathrm{i}\alpha z},\tag{16}$$

and similar transforms of $E^{(1,2,3,4)}_{\omega z}$, for example,

$$\Phi^{(1,2,3,4)}_{+}(\rho,\alpha)=(2\pi)^{-1}\int_0^{\infty}\mathrm{d}z\frac{k_0}{\mathrm{i}}E^{(1,2,3,4)}_{\omega z}(\rho,z)\,\mathrm{e}^{\mathrm{i}\alpha z}.\tag{17}$$

From Eqs. (17) and (2) we have the following relation between Φ and Ψ:

$$\Phi^{(1,2,3,4)}_{+}(\rho,\alpha)=\frac{\Psi^{(1,2,3,4)}_{+}(\rho,\alpha)}{\rho}+\frac{\partial\Psi^{(1,2,3,4)}_{+}(\rho,\alpha)}{\partial\rho},\tag{18}$$

and the same relation between $\Phi^{(4)}_{-}(\rho,\alpha)$ and $\Psi^{(4)}_{-}(\rho,\alpha)$.

From Eq. (14) we obtain

$$\Big(\frac{\partial^2}{\partial\rho^2}+\frac{1}{\rho}\frac{\partial}{\partial\rho}+\kappa^2-\frac{1}{\rho^2}\Big)\begin{Bmatrix}\Psi^{(1,2,3)}_{+}\\ \Psi^{(4)}_{-}+\Psi^{(4)}_{+}\end{Bmatrix}=\begin{Bmatrix}F^{(1,2,3)}\\ 0\end{Bmatrix},\tag{19}$$

$$2\pi F^{(1,2,3)}=\partial H^{(1,2,3)}_{\omega\varphi}/\partial z|_{z=0_+}-\mathrm{i}\alpha H^{(1,2,3)}_{\omega\varphi}|_{z=0_+},\tag{20}$$

where

$$\kappa=\sqrt{k_0^2-\alpha^2},\ \ \mathrm{Im}\kappa>0.\tag{21}$$

Equation (19) is obtained in a way similar to Eq. (9) in Ref. [17].

Functions $F^{(1,2,3)}$ are determined using the continuity of $E_{\omega\rho}$ and $H_{\omega\varphi}$ for $z=0$, $\rho<d$ (see Ref. [17] for details), therefore

$$2\pi F^{(1)}=\mathrm{i}\Big[(k_{zl}-\alpha)M^{(i)}J_1(\rho\sigma_l)/\sigma_l-\sum\nolimits_{m=1}^{\infty}(k_{zm}+\alpha)M_mJ_1(\rho\sigma_m)/\sigma_m\Big],\tag{22}$$

$$2\pi F^{(2)}=\mathrm{i}\Big[M^{(i)}\Big(\frac{k_{zl}}{\varepsilon}-\alpha\Big)\frac{J_1(b\sigma_l)}{\sigma_l}\frac{\psi_l(\rho)}{\psi_l(b)}-\sum_{m=1}^{\infty}M_m\Big(\frac{k_{zm}}{\varepsilon}+\alpha\Big)\frac{J_1(b\sigma_m)}{\sigma_m}\frac{\psi_m(\rho)}{\psi_m(b)}\Big],\tag{23}$$

$$2\pi F^{(3)}=\mathrm{i}\Big[M^{(i)}\Big(\frac{k_{zl}}{\epsilon}-\alpha\Big)\frac{J_1(b\sigma_l)}{\sigma_l}\frac{\psi_l(a)}{\psi_l(b)}\frac{\psi_{0l}(\rho)}{\psi_{0l}(a)}-\sum_{m=1}^{\infty}M_m\Big(\frac{k_{zm}}{\epsilon}+\alpha\Big)\frac{J_1(b\sigma_m)}{\sigma_m}\frac{\psi_m(a)}{\psi_m(b)}\frac{\psi_{0m}(\rho)}{\psi_{0m}(a)}\Big].\tag{24}$$

General solution to Eq. (19) has the form (see Ref. [17] for details):

$$\Psi_+^{(1)}(\rho,\alpha) = C^{(1)} J_1(\rho\kappa) + \Psi_p^{(1)}(\rho,\alpha), \tag{25}$$

$$\Psi_+^{(2)}(\rho,\alpha) = C_1^{(2)} J_1(\rho\kappa) + C_2^{(2)} Y_1(\rho\kappa) + \Psi_p^{(2)}(\rho,\alpha), \tag{26}$$

$$\Psi_+^{(3)}(\rho,\alpha) = C_1^{(3)} J_1(\rho\kappa) + C_2^{(3)} Y_1(\rho\kappa) + \Psi_p^{(3)}(\rho,\alpha), \tag{27}$$

$$\Psi_-^{(4)}(\rho,\alpha) + \Psi_+^{(4)}(\rho,\alpha) = C^{(4)} H_1^{(1)}(\rho\kappa), \tag{28}$$

where $H_\nu^{(1)}$ is a Hankel function of the first kind of ν-th order, $C^{(1,4)}$ and $C_{1,2}^{(2,3)}$ are unknown coefficients.

Particular solutions of the inhomogeneous equations $\Psi_p^{(1,2,3)}$ have the form (see Ref. [17] for details)

$$\Psi_p^{(1)}(\rho,\alpha) = \frac{\mathrm{i}M^{(i)}}{2\pi\sigma_l}\frac{J_1(\rho\sigma_l)}{k_{zl}+\alpha} - \sum_{m=1}^{\infty}\frac{\mathrm{i}M_m}{2\pi\sigma_m}\frac{J_1(\rho\sigma_m)}{k_{zm}-\alpha}, \tag{29}$$

$$\Psi_p^{(2)}(\rho,\alpha) = \frac{\mathrm{i}M^{(i)}}{2\pi}\frac{\frac{k_{zl}}{\varepsilon}-\alpha}{\kappa^2-s_l^2}\frac{J_1(b\sigma_l)}{\sigma_l}\frac{\psi_l(\rho)}{\psi_l(b)} - \sum_{m=1}^{\infty}\frac{\mathrm{i}M_m}{2\pi}\frac{\frac{k_{zm}}{\varepsilon}+\alpha}{\kappa^2-s_m^2}\frac{J_1(b\sigma_m)}{\sigma_m}\frac{\psi_m(\rho)}{\psi_m(b)}, \tag{30}$$

$$\Psi_p^{(3)}(\rho,\alpha) = \frac{\mathrm{i}M^{(i)}}{2\pi}\frac{\frac{k_{zl}}{\epsilon}-\alpha}{\kappa^2-\chi_l^2}\frac{J_1(b\sigma_l)}{\sigma_l}\frac{\psi_l(a)}{\psi_l(b)}\frac{\psi_{0l}(\rho)}{\psi_{0l}(a)} - \sum_{m=1}^{\infty}\frac{\mathrm{i}M_m}{2\pi}\frac{\frac{k_{zm}}{\epsilon}+\alpha}{\kappa^2-\chi_m^2}\frac{J_1(b\sigma_m)}{\sigma_m}\frac{\psi_m(a)}{\psi_m(b)}\frac{\psi_{0m}(\rho)}{\psi_{0m}(a)}. \tag{31}$$

From Eq. (18) one obtains the corresponding form of the general solution for Φ:

$$\Phi_+^{(1)}(\rho,\alpha) = \mathrm{i}k_0^{-1}C^{(1)}\kappa J_0(\rho\kappa) + \Phi_p^{(1)}(\rho,\alpha), \tag{32}$$

$$\Phi_+^{(2)}(\rho,\alpha) = \mathrm{i}k_0^{-1}C_1^{(2)}\kappa J_0(\rho\kappa) + \mathrm{i}k_0^{-1}C_2^{(2)}\kappa Y_0(\rho\kappa) + \Phi_p^{(2)}(\rho,\alpha), \tag{33}$$

$$\Phi_+^{(3)}(\rho,\alpha) = \mathrm{i}k_0^{-1}C_1^{(3)}\kappa J_0(\rho\kappa) + \mathrm{i}k_0^{-1}C_2^{(3)}\kappa Y_0(\rho\kappa) + \Phi_p^{(3)}(\rho,\alpha), \tag{34}$$

$$\Phi_-^{(4)}(\rho,\alpha) + \Phi_+^{(4)}(\rho,\alpha) = \mathrm{i}k_0^{-1}C^{(4)}\kappa H_0^{(1)}(\rho\kappa), \tag{35}$$

where

$$\Phi_p^{(1)}(\rho,\alpha) = \frac{-M^{(i)}}{2\pi k_0}\frac{J_0(\rho\sigma_l)}{k_{zl}+\alpha} + \sum_{m=1}^{\infty}\frac{M_m}{2\pi k_0}\frac{J_0(\rho\sigma_m)}{k_{zm}-\alpha}, \tag{36}$$

$$\Phi_p^{(2)}(\rho,\alpha) = \frac{-M^{(i)}}{2\pi k_0}\frac{\frac{k_{zl}}{\varepsilon}-\alpha}{\kappa^2-s_l^2}\frac{s_l J_1(b\sigma_l)}{\sigma_l}\frac{\phi_l(\rho)}{\phi_l(b)} + \sum_{m=1}^{\infty}\frac{M_m}{2\pi k_0}\frac{\frac{k_{zm}}{\varepsilon}+\alpha}{\kappa^2-s_m^2}\frac{s_m J_1(b\sigma_m)}{\sigma_m}\frac{\phi_m(\rho)}{\phi_m(b)}, \tag{37}$$

$$\Phi_p^{(3)}(\rho,\alpha) = \frac{-M^{(i)}}{2\pi k_0}\frac{\frac{k_{zl}}{\epsilon}-\alpha}{\kappa^2-\chi_l^2}\frac{J_1(b\sigma_l)}{\sigma_l}\frac{\psi_l(a)}{\psi_l(b)}\frac{\chi_l\phi_{0l}(\rho)}{\phi_{0l}(a)} + \sum_{m=1}^{\infty}\frac{M_m}{2\pi k_0}\frac{\frac{k_{zm}}{\varepsilon}+\alpha}{\kappa^2-\chi_m^2}\frac{J_1(b\sigma_m)}{\sigma_m}\frac{\psi_m(a)}{\psi_m(b)}\frac{\chi_m\phi_{0m}(\rho)}{\phi_{0m}(a)}, \tag{38}$$

where

$$\phi_{0m}(\rho) = J_0(\rho\chi_m)Y_0(d\chi_m) - Y_0(\rho\chi_m)J_0(d\chi_m),$$
$$\phi_m(\rho) = J_0(\rho s_m)\varphi_{2m} - Y_0(\rho s_m)\varphi_{1m}, \tag{39}$$

and $\Phi_p^{(3)}(d,\alpha) = 0$ since $\phi_{0m}(d) = 0$.

Boundary condition $E_{\omega z} = 0$ for $\rho = d$, $z < 0$ results in $\Phi_-^{(4)}(d,\alpha) = 0$, and we obtain from Eq. (35):

$$C^{(4)} = \frac{k_0\Phi_+^{(4)}(d,\alpha)}{\mathrm{i}\kappa H_1^{(1)}(d\kappa)}, \tag{40}$$

therefore from Eq. (28)

$$\Psi_+^{(4)}(d,\alpha) + \Psi_-^{(4)}(d,\alpha) = \frac{k_0\Phi_+^{(4)}(d,\alpha)H_1^{(1)}(d\kappa)}{\mathrm{i}\kappa H_1^{(1)}(d\kappa)}. \tag{41}$$

To obtain the Wiener–Hopf–Fock equation one should express the term $\Psi_+^{(4)}(d,\alpha)$ in Eq. (41) through the $\Phi_+^{(4)}(d,\alpha)$. This can be carried out using the continuity conditions for $\rho = b,a,d$, $z > 0$ (see Ref. [18] for details):

$$\begin{aligned}\Psi_+^{(4)}(d,\alpha) = {} & \frac{k_0\Phi_+^{(4)}(d,\alpha)J_1(d\kappa)}{\mathrm{i}\kappa J_0(d\kappa)} + \Psi_p^{(3)}(d,\alpha) \\ & - \frac{k_0}{\mathrm{i}\kappa d J_0(d\kappa)}\Big[bJ_1(b\kappa)(\Phi_p^{(1)}(b,\alpha) \\ & - \Phi_p^{(2)}(b,\alpha)) + aJ_1(a\kappa)(\Phi_p^{(2)}(a,\alpha) \\ & - \Phi_p^{(1)}(a,\alpha)) - \frac{\mathrm{i}b\kappa J_0(b\kappa)}{k_0}(\Psi_p^{(1)}(b,\alpha) \\ & - \Psi_p^{(2)}(b,\alpha)) - \frac{\mathrm{i}a\kappa J_0(a\kappa)}{k_0}(\Psi_p^{(2)}(a,\alpha) \\ & - \Psi_p^{(3)}(a,\alpha))\Big].\end{aligned} \tag{42}$$

Similar to Refs. [17,18], the right-hand side of Eq. (42) formally possesses pole singularity for $\alpha = \alpha_m$:

$$\alpha_m = \sqrt{k_0^2 - j_{0m}^2 d^{-2}}, \quad \mathrm{Im}\alpha_m > 0, \tag{43}$$

where j_{0m} is the m-th zero of the Bessel function J_0 (α_m are the longitudinal wavenumbers of a vacuum waveguide of radius d). However, the function determined by Eq. (42) should be regular in the area $\mathrm{Im}\alpha > -\delta$. Therefore, this pole singularity on the right-hand side should be eliminated and we obtain the following requirement:

$$\begin{aligned}& \Phi_+^{(4)}(d,\alpha_p)J_1(j_{0p}) \\ & = \frac{1}{d}\Big\{bJ_1(bj_{0p}/d) \\ & \quad \times [\Phi_p^{(1)}(b,\alpha_p) - \Phi_p^{(2)}(b,\alpha_p)] \\ & \quad + aJ_1(aj_{0p}/d)[\Phi_p^{(2)}(a,\alpha_p) - \Phi_p^{(1)}(a,\alpha_p)] \\ & \quad - \frac{\mathrm{i}bj_{0p}J_0(bj_{0p}/d)}{dk_0}[\Psi_p^{(1)}(b,\alpha_p) - \Psi_p^{(2)}(b,\alpha_p)] \\ & \quad - \frac{\mathrm{i}aj_{0p}J_0(aj_{0p}/d)}{dk_0}[\Psi_p^{(2)}(a,\alpha_p) - \Psi_p^{(3)}(a,\alpha_p)]\Big\}.\end{aligned} \tag{44}$$

Substituting Eq. (42) into Eq. (41) and combining the terms proportional to $\Phi_+^{(4)}(d,\alpha)$ we obtain the following Wiener–Hopf–Fock equation:

$$\frac{2k_0\Phi_+^{(4)}(d,\alpha)}{\kappa G(\alpha)}+\Psi_-^{(4)}(d,\alpha)+\frac{1}{dJ_0(d\kappa)}\frac{\mathrm{i}}{2\pi}\Pi(\alpha)=0, \quad (45)$$

where

$$G(\alpha)=\pi d\kappa J_0(d\kappa)H_0^{(1)}(d\kappa), \quad (46)$$

$$\begin{aligned}\Pi(\alpha)=&\,b\frac{M^{(i)}\zeta_{1l}(\alpha)}{k_{zl}+\alpha}-\sum_{m=0}^{\infty}b\frac{M_m\zeta_{1m}(\alpha)}{k_{zm}-\alpha}\\&+M^{(i)}\frac{\frac{k_{zl}}{\varepsilon}-\alpha}{\kappa^2-s_l^2}\frac{s_lJ_1(b\sigma_l)}{\sigma_l\psi_l(b)}\eta_{1l}(\alpha)\\&-\sum_{m=0}^{\infty}M_m\frac{\frac{k_{zm}}{\varepsilon}+\alpha}{\kappa^2-s_m^2}\frac{s_mJ_1(b\sigma_m)}{\sigma_m\psi_m(b)}\eta_{1m}(\alpha)\\&+aM^{(i)}\frac{\frac{k_{zl}}{\epsilon}-\alpha}{\kappa^2-\chi_l^2}\frac{J_1(b\sigma_l)}{\sigma_l}\frac{\psi_l(a)}{\psi_l(b)\psi_{0l}(a)}\eta_{2l}(\alpha)\\&-\sum_{m=0}^{\infty}aM_m^{(i)}\frac{\frac{k_{zm}}{\epsilon}+\alpha}{\kappa^2-\chi_m^2}\frac{J_1(b\sigma_m)}{\sigma_m}\frac{\psi_m(a)}{\psi_m(b)\psi_{0m}(a)}\eta_{2m}(\alpha),\end{aligned} \quad (47)$$

$$\begin{aligned}\eta_{1m}(\alpha)=&\,b\phi_{2m}\mu_{bm}(\alpha)-a\phi_{2m}\mu_{am}(\alpha)\\&-b\phi_{1m}\nu_{bm}(\alpha)+a\phi_{1m}\nu_{am}(\alpha),\\\mu_{bm}(\alpha)=&\,J_0(b\kappa)J_1(bs_m)/s_m-J_0(bs_m)J_1(b\kappa)/\kappa,\\\nu_{bm}(\alpha)=&\,J_0(b\kappa)Y_1(bs_m)/s_m-Y_0(bs_m)J_1(b\kappa)/\kappa,\\\mu_{am}(\alpha)=&\,J_0(a\kappa)J_1(as_m)/s_m-J_0(as_m)J_1(a\kappa)/\kappa,\\\nu_{am}(\alpha)=&\,J_0(a\kappa)Y_1(as_m)/s_m-Y_0(as_m)J_1(a\kappa)/\kappa,\\\eta_{2m}(\alpha)=&\,\chi_mY_0(d\chi_m)\zeta_{2m}+J_0(d\chi_m)(\chi_mJ_1(a\kappa)Y_0(a\chi_m)/\kappa\\&-J_0(a\kappa)Y_1(a\chi_m))-2J_0(d\kappa)(\pi a\chi_m)^{-1},\\\zeta_{1m}(\alpha)=&\,J_0(b\sigma_m)J_1(b\kappa)/\kappa-J_0(b\kappa)J_1(b\sigma_m)/\sigma_m.\end{aligned} \quad (48)$$

Equation (45) is solved in a common way (see Refs. [17, 18,21] for details). Omitting standard factorizations and estimations, we obtain

$$\begin{aligned}\Phi_+^{(4)}(d,\alpha)=&\,\frac{1}{4\pi\mathrm{i}k_0d}\kappa_+(\alpha)G_+(\alpha)\\&\times\sum_{q=1}^{\infty}\Pi(-\alpha_q)\frac{\kappa_+(\alpha_q)G_+(\alpha_q)j_{0q}}{d^2\alpha_qJ_1(j_{0q})(\alpha+\alpha_q)}.\end{aligned} \quad (49)$$

To find $\{M_m\}$, one should substitute Eq. (49) into Eq. (44). After transformations, we obtain an infinite linear system in the form

$$\sum_{m=1}^{\infty}W_{pm}M_m=M^{(i)}w_p,\quad p=1,2,\ldots, \quad (50)$$

which is convergent and can be solved numerically using the reducing technique (see, for example, Refs. [17,18] for details).

When the set of coefficients $\{M_m\}$ is determined, the electromagnetic field can be calculated via the inverse transform over α, in accordance with Eqs. (15) and (16):

$$H_{\omega\varphi}^{(1,2,3)}(\rho,z>0)=\int_{-\infty}^{+\infty}\Psi_+^{(1,2,3)}(\rho,\alpha)\,\mathrm{e}^{-\mathrm{i}\alpha z}\,\mathrm{d}\alpha, \quad (51)$$

$$H_{\omega\varphi}^{(4)}(\rho,z)=\int_{-\infty}^{+\infty}\Psi^{(4)}(\rho,\alpha)\,\mathrm{e}^{-\mathrm{i}\alpha z}\,\mathrm{d}\alpha. \quad (52)$$

Performing calculations similar to those in Ref. [18], one obtains that the field in the region $z>0$ is described by the unified formula:

$$H_{\omega\varphi}^{(1,2,3,4)}(\rho,z>0)=\sum_{q=1}^{\infty}\Pi(-\alpha_q)\frac{\kappa_+(\alpha_q)G_+(\alpha_q)j_{0q}}{d^2\alpha_qJ_1(j_{0q})}\frac{L_q^+(\rho,z)}{2}, \quad (53)$$

where L_q^+ is given by Eq. (47) in Ref. [17].

For the domain 4, one can also obtain the representation convenient for investigation of the far field:

$$H_{\omega\varphi}^{(4)}(\rho,z)=\frac{1}{d}\sum_{q=1}^{\infty}\Pi(-\alpha_q)\frac{\kappa_+(\alpha_q)G_+(\alpha_q)j_{0q}}{d^2\alpha_qJ_1(j_{0q})}\frac{I_q^{(4)}}{4\pi}, \quad (54)$$

where integral

$$I_q^{(4)}(\rho,z)=\int_{-\infty}^{+\infty}\frac{\kappa_+(\alpha)G_+(\alpha)H_1^{(1)}(\rho\kappa)}{\kappa(\alpha)H_0^{(1)}(a\kappa)(\alpha_q+\alpha)}\,\mathrm{e}^{-\mathrm{i}\alpha z}\,\mathrm{d}\alpha \quad (55)$$

has been investigated before [see Eq. (41) in Ref. [17]]. In particular, integral (55) can be easily calculated asymptotically, see Eq. (51) in Ref. [17] and Eq. (8) in this paper, and we can substitute integral (55) into Eq. (54) to obtain the far field in region 4.

5. Conclusion

We have presented a convenient rigorous approach for calculating various diffraction processes at the open end (with orthogonal cut) of a circular waveguide with a three-layer dielectric lining. In other words, we have rigorously solved the corresponding canonical diffraction problem. In this paper, we have considered the specific case of excitation in the form of a symmetric TM waveguide mode. However, this approach can be extended to more complicated problems, for example, excitation by a charged particle bunch (in full formulation including both wakefield radiation and diffraction radiation) could be included in the solution.

The obtained solution has been applied for investigation of radiation of Cherenkov wakefield from the open-ended three-layer capillary suggested in Ref. [13] as a promising structure for realization of beam-driven THz source with small divergence and high efficiency. While paper Ref. [13] dealt with the case where only a fundamental Cherenkov mode is excited and radiated, our analytic approach has allowed consideration of high-order Cherenkov modes. In this case, THz

radiation frequencies can be obtained for mm-sized (not sub-mm) capillaries, which are more favorable in fabrication. It has been shown that for a enough thick third layer with permittivity slightly larger than unity, a single-lobe radiation pattern with low reflection can be achieved. Additionally, the angle of the main lobe decreases with an increase in the number of excited Cherenkov modes.

Acknowledgments

This work was supported by the Russian Science Foundation (Grant No. 18-72-10137). Authors are grateful to S. S. Baturin for fruitful discussion.

References

[1] Nanni E A, Huang W R, Hong K H, Ravi K, Fallahi A, Moriena G, Dwayne Miller R J and Kärtner F X 2015 *Nat. Commun.* **6** 8486
[2] O'Shea D B, Andonian G, Barber S, Fitzmorris K, Hakimi S, Harrison J, D Hoang P, J Hogan M, Naranjo B, B Williams O, Yakimenko V and Rosenzweig J 2016 *Nat. Commun.* **7** 12763
[3] Wang D, Su X, Yan L, Du Y, Tian Q, Liang Y, Niu L, Huang W, Gai W, Tang C and Antipov S 2017 *Appl. Phys. Lett.* **111** 174102
[4] Jing C, Antipov S, Conde M, Gai W, Ha G, Liu W, Neveu N, Power J, Qiu J, Shi J, Wang D and Wisniewski E 2018 *Nucl. Instrum. Methods Phys. Res. Sect. A* **898** 72
[5] Hibberd M T, Healy A L, Lake D S, Georgiadis V, Smith E J H, Finlay O J, Pacey T H, Jones J K, Saveliev Y, Walsh D A, Snedden E W, Appleby R B, Burt G, Graham D M and Jamison S P 2020 *Nat. Photon.* **14** 755
[6] Tang H, Zhao L, Zhu P, Zou X, Qi J, Cheng Y, Qiu J, Hu X, Song W, Xiang D and Zhang J 2021 *Phys. Rev. Lett.* **127** 074801
[7] Galyamin S N, Tyukhtin A V, Antipov S and Baturin S S 2014 *Opt. Express* **22** 8902
[8] Ivanyan M, Grigoryan A, Tsakanian A and Tsakanov V 2014 *Phys. Rev. ST Accel. Beams* **17** 074701
[9] Wang D, Su X, Du Y, Tian Q, Liang Y, Niu L, Huang W, Gai W, Yan L, Tang C and Antipov S 2018 *Rev. Sci. Instrum.* **89** 093301
[10] Zhao L, Tang H, Lu C, Jiang T, Zhu P, Hu L, Song W, Wang H, Qiu J, Jing C, Antipov S, Xiang D and Zhang J 2020 *Phys. Rev. Lett.* **124** 054802
[11] Altmark A, Lesiv N and Mukhamedgaliev K 2019 *J. Phys.: Conf. Ser.* **1145** 012039
[12] Antipov S, Spentzouris L, Gai W, Conde M, Franchini F, Konecny R, Liu W, Power J G, Yusof Z and Jing C 2008 *J. Appl. Phys.* **104** 014901
[13] Jiang S, Li W, He Z, Jia Q and Wang L 2020 *Opt. Lett.* **45** 5416
[14] Altmark A M, Kanareykin A D and Sheinman I L 2005 *Tech. Phys.* **50** 87
[15] Jing C, Kanareykin A, Power J G, Conde M, Liu W, Antipov S, Schoessow P and Gai W 2011 *Phys. Rev. Lett.* **106** 164802
[16] Bilyk V R and Grishunin K A 2019 *Russian Technol. J.* **7** 71
[17] Galyamin S N, Vorobev V V and Tyukhtin A V 2021 *IEEE Trans. Microw. Theory Tech.* **69** 2429
[18] Galyamin S N and Vorobev V V 2022 *IEEE Trans. Microw. Theory Tech.* **70** 3087
[19] Galyamin S N, Tyukhtin A V, Vorobev V V, Grigoreva A A and Aryshev A S 2019 *Phys. Rev. Accel. Beams* **22** 012801
[20] Weinstein L 1969 *The Theory of Diffraction and the Factorization Method: Generalized Wiener-Hopf Technique* Golem Series in Electromagnetics **3** (Golem Press)
[21] Mittra R and Lee S 1971 *Analytical Techniques in the Theory of Guided Waves* (Macmillian)
[22] Williams W E and Lighthill M J 1956 *Mathematical Proceedings of the Cambridge Philosophical Society* **52** 322
[23] Voskresenskii G and Zhurav S 1978 *Radiotekhnika i Electronika* **23** 2505
[24] Johnson T and Moffatt D 1980 *Electromagnetic scattering by open circular waveguides* Technical Report 710816-9 (The Ohio State University)
[25] Kobayashi K 1991 *Antennas and Propagation Society Symposium 1991 Digest*, London, ON, Canada, June 24–28, 1991, vol. 2 pp. 1054–1057
[26] Kobayashi K and Sawai A 1992 *J. Electromagn. Waves Appl.* **6** 475
[27] Koshikawa S and Kobayashi K 1997 *IEEE Trans. Antenn. Propagat.* **45** 949
[28] Gupta S, Bhattacharya A and Chakraborty A 1997 *IEE Proceedings - Microwaves, Antennas and Propagation* **144** 126
[29] Kuryliak D, Koshikawa S, Kobayashi K and Nazarchuk Z 2000 *Conference Proceedings 2000 International Conference on Mathematical Methods in Electromagnetic Theory (Cat. No.00EX413)*, September 12–15, 2000, Kharkov, Ukraine, vol. 2 p. 694
[30] Kuryliak D B, Kobayashi K, Koshikawa S and Nazarchuk Z T 2004 *10th International Conference on Mathematical Methods in Electromagnetic Theory*, September 14–17, 2004, Dniepropetrovsk, Ukraine, p. 251
[31] Hameş Y and Tayyar I H 2004 *Prog. Electromagnet. Res.* **44** 143
[32] Hameş Y and Tayyar I H 2005 *Electromagnetics* **25** 245
[33] Cicchetti R and Faraone A 2008 *Prog. Electromagnet. Res.* **78** 285
[34] Galyamin S N, Tyukhtin A V and Vorobev V V 2017 *Nucl. Instrum. Methods Phys. Res. Sect. B* **402** 144
[35] Buyukaksoy A, Tayyar I H, Hacivelioglu F and Uzgoren G 2007 2007 *International Conference on Electromagnetics in Advanced Applications*, September 17–21, 2007, Turin, Italy, p. 649
[36] Buyukaksoy A, Hacivelioglu F and Uzgoren G 2008 *12th International Conference on Mathematical Methods in Electromagnetic Theory*, June 29, 2008–July 02, 2008, Odessa, Ukraine, p. 85
[37] Hacivelioglu F, Buyukaksoy A, Uzgoren G and Serbest H 2009 *Mediterrannean Microwave Symposium (MMS)*, November 15–17, 2009, Tangiers, Morocco, p. 1
[38] Tayyar I H and Buyukaksoy A 2011 *International Conference on Electromagnetics in Advanced Applications*, September 12–16, 2011, Turin, Italy, p. 580
[39] Zaki K and Atia A 1983 *IEEE Trans. Microw. Theory Tech.* **31** 1039
[40] Zaki K, Seng-Woon C and Chunming C 1988 *IEEE Trans. Microw. Theory Tech.* **36** 1804
[41] Bolotovskii B M 1962 *Sov. Phys. Usp.* **4** 781
[42] Antipov S, Baryshev S, Jing C, *et al.* 2015 *Proceedings of the 6th International Particle Accelerator Conference (IPAC2015)*, May 3–8, 2015, Greater Richmond Convention Center in Richmond, VA, USA, p. 1029